Short summary of the PhD thesis defense and analysis of $Z^{'}$

Mohamed Gouighri
Abdeslam Hoummada

Mohamed.Gouighri@cern.ch

University Hassan II of Casablanca

June 18, 2012

A brief summary of my doctoral thesis

- The PhD thesis was on "**Electronic calibration of the ATLAS liquid argon calorimeter and analysis of $B_d^0 \to J/\psi(\mu\mu)K_s^0(\pi\pi)$ and $\Lambda_b \to J/\psi(\mu\mu)\Lambda^0(p\pi)$ channels with the first LHC data**"
- Defended on the 23^{rd} January 2012
- Before the committee comprised of:

Pr: O. Fassi-Fehri	Mohamed V University	President
Pr: P. Fassnacht	CERN	Examinateur
Pr: A. Arhrib	AbdelMalek Essadi University	Rapporteur
Pr: J. Collot	LPSC of Grenoble	Rapporteur
Pr: D. Benchekroun	University of Casablanca	Rapporteur
Pr: G. Unal	CERN	Supervisor CERN
Pr: E. Bouhova-Thacker	Lancaster University	Supervisor CERN
Pr: A. Hoummada	University of Casablanca	Supervisor
Pr: R. Klapisch	Sharing Knowledge Foundation	Invited
Pr: G. Carnot	Carnot Foundation	Invited

Overview and the Motivation

The thesis focused in two main parts:

- **Experimental Part:** Dedicated to the electronic calibration of the ATLAS Liquid Argon (LAr) calorimeters
  - To provide high-quality of data ready for physics analysis, the calibration and alignment of the detector is highly crucial
    - Monitor the electronics readout system, its linearity and stability over time through dedicated calibration runs
  - The computation of energy deposit in a LAr cell
  - The techniques for the automatic processing of the calibration chain and how the calibration of the detectors is validated
- **Physics Part:** The topic is the B-physics analysis
  - Two most interesting channels are fully reconstructed and analyzed, $B_d^0 \to J/\psi(\mu^+\mu^-)K_S^0(\pi^+\pi^-)$ and $\Lambda_b^0 \to J/\psi(\mu^+\mu^-)\Lambda^0(p\pi)$
  - The $B_d^0 \to J/\psi(\mu^+\mu^-)K_S^0(\pi^+\pi^-)$ is a clean channel to measure the CP violation parameters ($\sin 2\beta$)
  - Hadron colliders such as the LHC are the only facilities where the properties of b-baryons can be studied
  - The lifetime ratio $\frac{\tau_{\Lambda_b}}{\tau_{B_d}}$, helicity and polarization of $\Lambda_b/\bar{\Lambda}_b$ is of great theoretical interest (predicted by HQET and pQCD)

Overview and the Motivation

The thesis focused in two main parts:

- **Experimental Part:** Dedicated to the electronic calibration of the ATLAS Liquid Argon (LAr) calorimeters
  - To provide high-quality of data ready for physics analysis, the calibration and alignment of the detector is highly crucial
    - Monitor the electronics readout system, its linearity and stability over time through dedicated calibration runs
  - The computation of energy deposit in a LAr cell
  - The techniques for the automatic processing of the calibration chain and how the calibration of the detectors is validated
- **Physics Part:** The topic is the B-physics analysis
  - Two most interesting channels are fully reconstructed and analyzed, $B_d^0 \to J/\psi(\mu^+\mu^-)K_S^0(\pi^+\pi^-)$ and $\Lambda_b^0 \to J/\psi(\mu^+\mu^-)\Lambda^0(p\pi)$
  - The $B_d^0 \to J/\psi(\mu^+\mu^-)K_S^0(\pi^+\pi^-)$ is a clean channel to measure the CP violation parameters ($\sin 2\beta$)
  - Hadron colliders such as the LHC are the only facilities where the properties of b-baryons can be studied
  - The lifetime ratio $\frac{\tau_{\Lambda_b}}{\tau_{B_d}}$, helicity and polarization of $\Lambda_b/\bar{\Lambda}_b$ is of great theoretical interest (predicted by HQET and pQCD)

Calibration of the ATLAS LAr Calorimeters

Energy Reconstruction and Calibration

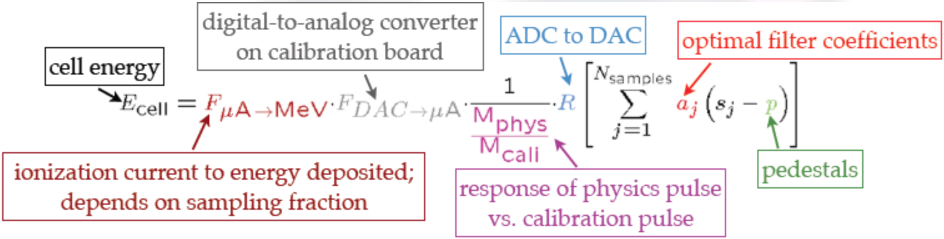

- There are regular calibration runs (Pedestal, Ramp and Delay) taken.
  - Pedestal: determines pedestal value, noise (from RMS of pedestal)
  - Ramp: determines gain of readout from slope of reconstructed pulse amplitude vs. DAC setting
  - Delay: fixed-amplitude pulses injected; effective sampling rate of 1 ns
- These are used to update (if needed) the calibration constants in the database.

LAr Calibration Stability

- The investigation into the stability of the constants is essential for a good calorimeter performance
- Stability of constants monitored over extended periods of time (plots show a 6-month period in early 2009)

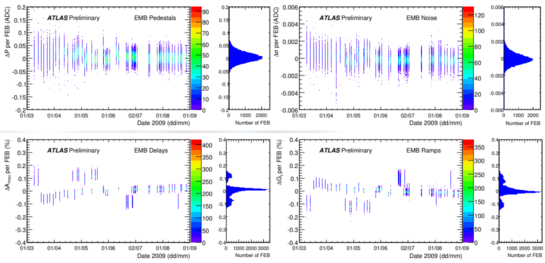

- Pedestal: $<$ 0.1 ADC count for all calorimeters
- Noise: $<$ 0.002 ADC count for all calorimeters
- Gain: $<$ 0.2% for all calorimeters
- Delay: $<$ 0.2% for all calorimeters

- **Robust calibration procedure**
- **Good electronic stability**

The CrossTalk Correction

Motivation: The Electromagnetic Calorimeter cells share a part of their collected current via: capacitances in Sampling 1, HV ink resistors collect S1 and S2, or via mutual inductances S2, S3.

- Normally, precautions are taken for channels having known bad neighbours but participating in the energy computation
- We added a codding part to the LArCalibUtils package to take into account this effect.

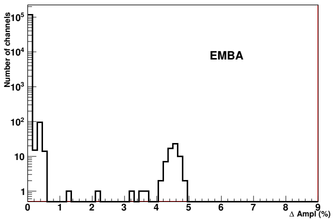

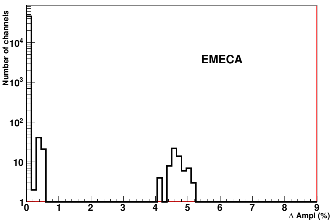

Physics Analysis

Introduction

- Analysis of $B_d^0 \to J/\psi(\mu^+\mu^-)K_S^0(\pi^+\pi^-)$:
  - Physics interests: lifetime, CP Violation, cross-section
  - Status: Observation note with 2010 data approved, lifetime measurement, CP-violation measurements (ongoing work)
- Analysis of $\bar{\Lambda}_b^0 \to J/\psi(\mu^+\mu^-)\bar{\Lambda}(p^{+(-)}\pi^{-(+)})$:
  - Physics interests: lifetime, B_d^0/Λ_b^0 lifetime ratio, helicity amplitudes and polarization
  - Status: Observation note with 2011 data approved, paper on the lifetime measurement, working on the polarization and helicity amplitudes
- Jpsi+V0 analysis software official as part of ATHENA software (DAOD framework)

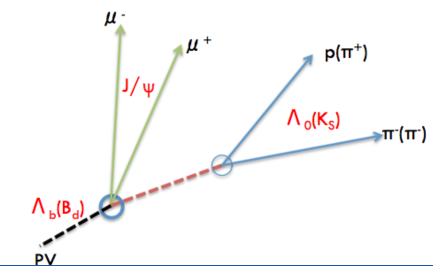

Data

Real Data:

- Data: 2010 November reprocessed data, Integrated luminosity 40 pb^{-1}
- Data: 2011 November reprocessed data, periods B2-H, Integrated luminosity 1.2 fb^{-1}
- Data: 2011 November reprocessed data, Integrated luminosity 5 fb^{-1} (For $\Lambda_b/\bar{\Lambda}_b$ lifetime)
- GRL: data10_7TeV.pro05.merged_LBSUMM_muon_7TeV.xml
- GRL: data11_7TeV.periodAllYear_DetStatus-v22-pro08-06_CoolRunQuery-00-03-98_Muon.xml

Monte Carlo:

Sample	No. of events	Generator-level μ cuts	σ
$B_d^0 \to J/\psi(\mu^+\mu^-)K_S^0(\pi^+\pi^-)$	500k	$p_T^{\mu_1(\mu_2)} > 2.5(0)$ GeV	5.64 nb
$\bar{\Lambda}_b^0 \to J/\psi(\mu^+\mu^-)\bar{\Lambda}(p^{+(-)}\pi^{-(+)})$	500k	$p_T^{\mu_1(\mu_2)} > 2.5(0)$ GeV	0.031 nb
Inclusive direct $J/\psi(\mu^+\mu^-)X$	1M	$p_T^{\mu 1,2} > 2.5$ GeV	425 nb
Inclusive $b\bar{b} \to J/\psi(\mu^+\mu^-)X$	1M	$p_T^{\mu 1,2} > 2.5$ GeV	55.68 nb
Inclusive $b\bar{b} \to \mu^+\mu^-X$	2M	$p_T^{\mu 1,2} > 2.5$ GeV	509 nb
Inclusive $c\bar{c} \to \mu^+\mu^-X$	2M	$p_T^{\mu 1,2} > 2.5$ GeV	166 nb

Table: Signal and background Monte Carlo samples

- Signal events are removed from the backround ones
- Events containing $b \to J/\psi X$ decays are removed from the $b\bar{b} \to \mu^+\mu^-X$ sample
- Events containing a b-quark are removed from the $c\bar{c} \to \mu^+\mu^-X$ sample
- Samples are weighted by the corresponding cross-section

Results: B_d^0 Mass Fit $\quad M_{B_d^0}^{PDG} = 5279.5$ MeV

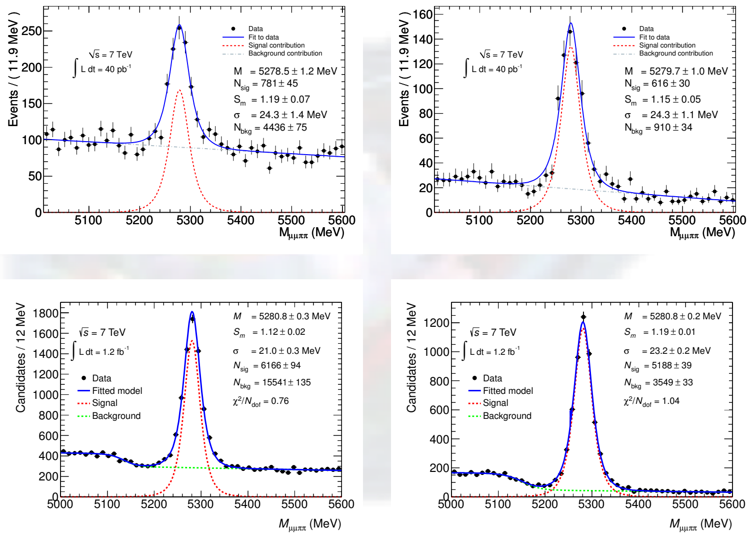

Distribution of the invariant mass of B_d^0 candidates reconstructed in 2010 data (top) and 2011 (bottom) without a proper decay time cut (left) and after the decay time cut of 0.35 ps (right)

Results: Lifetime Fit $\tau_{B_d^0} = 1.519 \pm 0.007$ ps

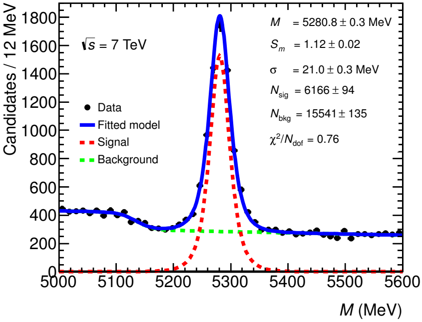

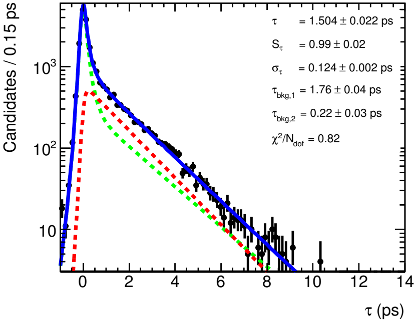

- B_d^0 mass: 5280.8 $\pm$ 0.3 (stat) MeV
- B_d^0 lifetime: 1.504 $\pm$ 0.022 (stat) $\pm$ 0.042(syst) ps

Results: Lifetime Fit

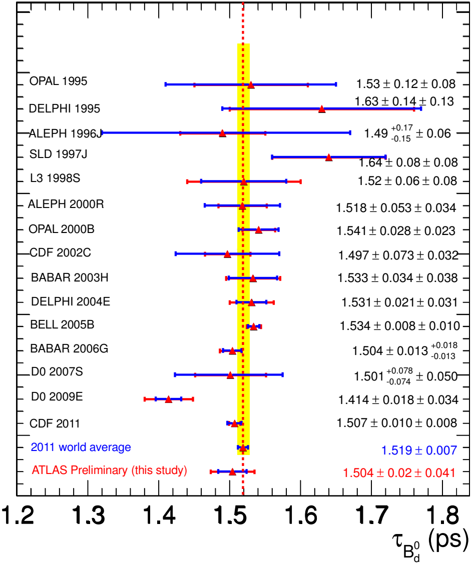

Results: $\Lambda_b/\bar{\Lambda}_b$ Mass Fit $M^{PDG}_{\Lambda^0_b} = 5620.2$ MeV

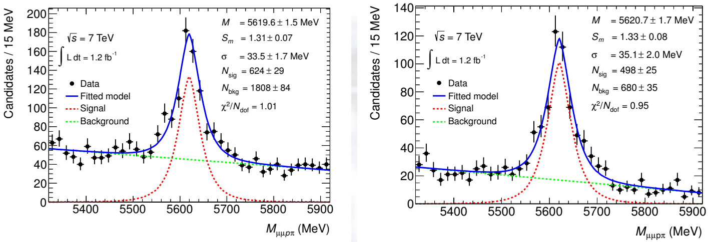

Distribution of the invariant mass of $\Lambda_b/\bar{\Lambda}_b$ candidates reconstructed with 1.2 fb^{-1} of 2011 data without a proper decay time cut (left) and after the proper decay time cut of 0.35 ps (right)

	1.2 fb^{-1} of 2011 Data	
Parameter	No proper decay time cut	$\tau_{\Lambda_b/\bar{\Lambda}_b} > 0.35$ ps
M (MeV)	5619.6 ± 1.5	5620.7 ± 1.7
S_m	1.31 ± 0.07	1.33 ± 0.08
$N_{\rm sig}$	624 ± 29	498 ± 25
$N_{\rm bkg}$	1808 ± 84	680 ± 35
σ_m (MeV)	33.5 ± 1.7	35.1 ± 2.0
Fit $\chi^2/N_{\rm d.o.f.}$	1.01	0.95

Table: Results of the $\Lambda^0_b/\bar{\Lambda}^0_b$ mass fits with 1.2 fb^{-1} of data. The listed errors are statistical only

Results: Lifetime Fit $\tau_{\Lambda_b^0} = 1.445 \pm 0.01$ ps

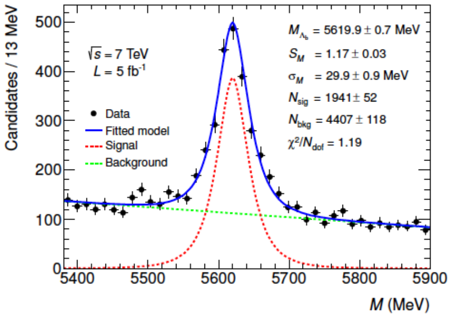

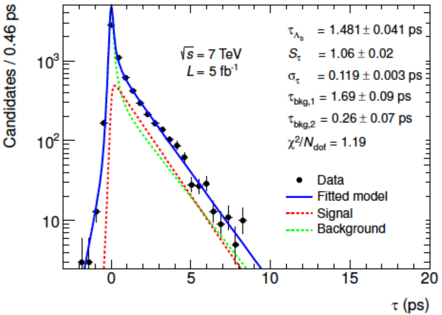

Fitted parameter	
Λ_b^0 mass, M_{Λ_b}	5619.9 ± 0.7(stat) MeV
Uncorrected Λ_b^0 lifetime, τ_{Λ_b}	1.481 ± 0.041(stat) ps
Signal fraction, f_{sig}	0.306 ± 0.008
Mass error scale factor, S_M	1.17 ± 0.03
Proper decay time error scale factor, S_τ	1.06 ± 0.02
Fit quality, χ^2/N_{dof}	1.19
Calculated parameters	
Corrected Λ_b^0 lifetime, $\tau^*_{\Lambda_b}$	1.461 ± 0.042(stat) ps
Number of signal candidates, N_{sig}	1941 ± 52
Number of background candidates, N_{bkg}	4407 ± 118
Mass resolution, σ_M	29.9 ± 0.9
Proper decay time resolution, σ_τ	0.119 ± 0.003

Results: Lifetime Fit

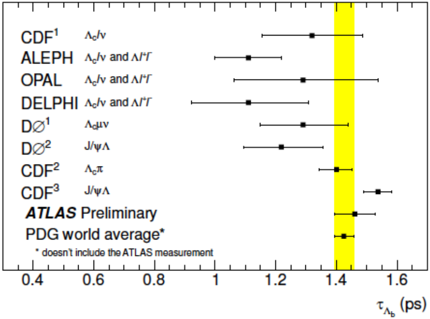

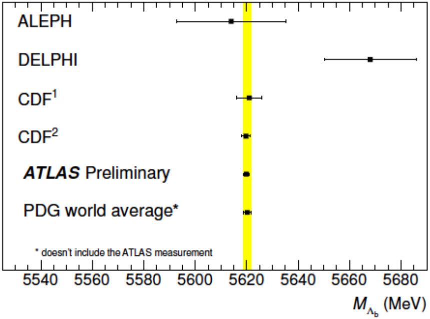

- Shown error bars are the combination of statistical and systematic errors.

- Λ_b^0 mass: 5619.9 $\pm$ 0.7 (stat) MeV
- Λ_b^0 lifetime: 1.461 $\pm$ 0.042 (stat) $\pm$ 0.052(syst) ps

Z' analysis

Recently joined the exotics ATLAS group and work on the $Z^{'} \rightarrow ee$

Ongoing work on the $Z' \rightarrow \mu\mu$ by Said Lablak

$Z' \rightarrow ee$ Status:

- The analysis code is in place and works on MC and 2012 Data
- Working on the Cut flow optimization.
- Reweithing between 7 TeV and 8 TeV MC data
- Test different models is ongoing using a validated release (17.2.4.2) with ZPRIMEee against SMWZ Ntuples

Results are coming in the next few days and will be presented on the next ILCP meeting

Conclusions and Perspectives

- Experimental Part:
  - Several years of commissioning with test beams, calibration, cosmic muons and now LHC collisions, ATLAS Liquid Argon Calorimeters are approaching the optimized working point:
    - Calibration system, including ionization pulse model, well understood
    - The studies performed using ATLAS data show that the LAr Calorimeters are performing well. The performances are well understood and close to the design expectation
  - After 10 years of operation and with the sLHC expected radiation level, an upgrade to the front end electronics will be necessary
    - this provides an opportunity to modernize components and revise the architecture
- Physics Part:
  - $B_d^0 \to J/\psi(\mu^+\mu^-)K_S^0(\pi^+\pi^-)$ and $\bar{\Lambda}_b^0 \to J/\psi(\mu^+\mu^-)\bar{\Lambda}(p^{+(-)}\pi^{-(+)})$ are fully reconstructed and analyzed using first LHC data
  - Mass and propertime consistent with the world average values
  - Validation of the reconstruction technique of this cascade decays in place for physics measurements (CP violation, helicity amplitudes, polarization)
  - Ongoing work on CP violation, helicity amplitudes, polarization
  - The Z' analysis is ongoing

Thanks For Your Attention

Backup slides

Calibration Constants Computation

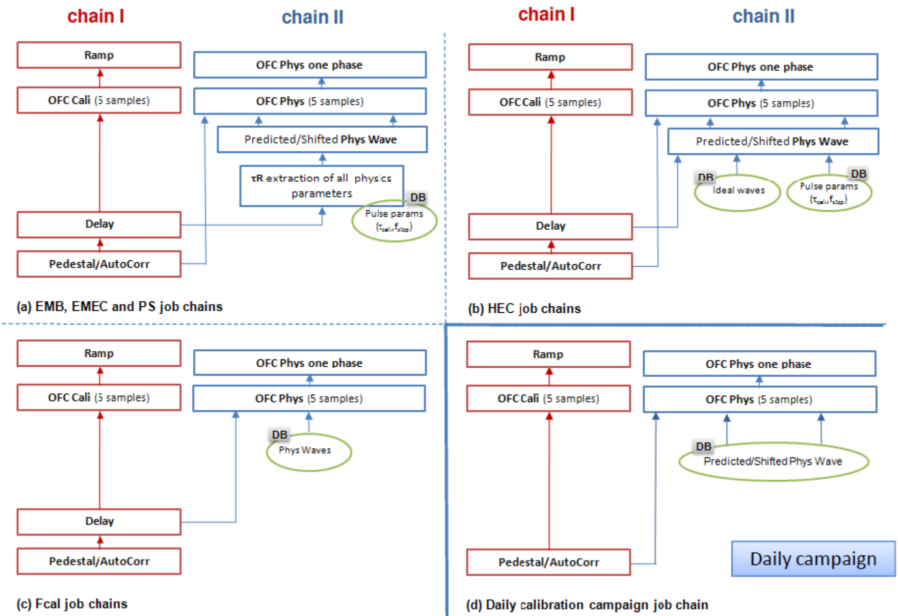

Automatic Processing - ECAL team

- To have a fast turnaround time between calibration runs and the availability of computed constants, much of the reconstruction and validation of LAr calibration runs has been automated in a software package referred to as the Automatic Processing (AP).
- We strongly participated to its development by:
  - Cross-check with experts the results from the AP and the results by running the codes on lxplus.
  - Development of part of AP jobOptions.
- The ECAL team was formed to monitor the stability of the calibration constants by investigating the output of the AP which include:
  - log from the Validation Tools,
  - ntuples from the constant dumpers, which allow us to compare each value of the calibration constant in a cell with a reference value
- As well, the team investigates any other issue related to electronic calibration that arises.

The Validation Tools needed proper thresholds in order to work properly and allow us to “see” problematic channels.

LAr Temperature Stability

- Variations of the liquid argon temperature have a direct impact on the readout signal, and consequently on the energy scale
  - the stability of the electronics temperature from June 22, 2009 to July 7, 2009 is presented

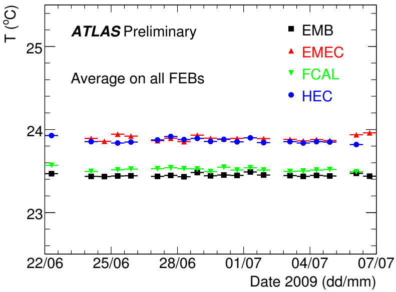

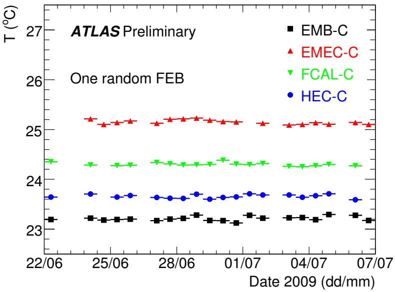

The CrossTalk Study

- CrossTalk: arises when the signal flows from one cell which records a physical signal in the other cells
- The crosstalk is measured by pulsing a channels and reading the others
  - **Capacitive:** the coupling capacitance between cells
  - **Resistive:** large “ink resistors” on the kapton electrodes
  - **Inductive:** the mutual inductance between the cells and from the ground return
- Two definitions:
  - **The Peak-to-peak definition** = V'_{max} / V_{max}
  - **The Under-the-peak definition** = $V'(T_{max}) / V_{max}$

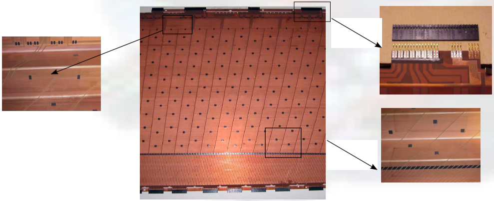

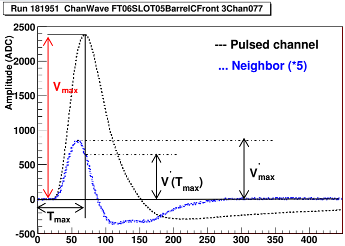

The CrossTalk Study

- In general the effect is negligible, and anyway compensated by the clustering algorithm

But, the effect is non negligible for the first sampling (front compartment a.k.a. Strips)

$$\frac{X}{V} \propto \frac{C_X}{C_d + 2C_X}$$

- The actual electronic gain is overestimated (∼9%)
- The pulse shapes obtained injecting the calibration current are “wrong” w.r.t. the one generated by a particle shower (cluster)

Schematic of the capacitive crosstalk between two neighbour channel

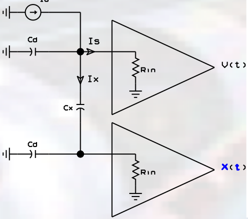

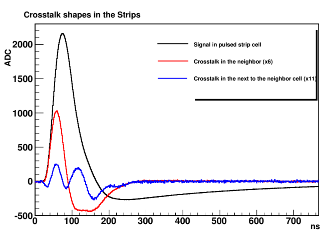

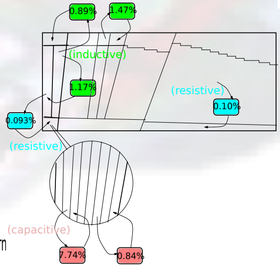

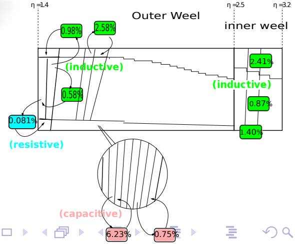

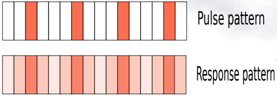

Physics Analysis

Reconstruction Strategy

Reconstruction of $B_d^0 \to J/\psi(\mu^+\mu^-)K_S^0(\pi^+\pi^-)$ and $\bar{\Lambda}_b^0 \to J/\psi(\mu^+\mu^-)\bar{\Lambda}(p^{+(-)}\pi^{-(+)})$

1. $J/\psi \to \mu^+\mu^-$ reconstruction: JpsiFinder, provides pairs of vertex-refitted muons and the J/ψ vertex (mass unconstrained vertex fit)
2. $K_S^0 \to \pi^+\pi^-$ and $\bar{\Lambda}(p^{+(-)}\pi^{-(+)})$: V0Finder, provides pairs of vertex-refitted tracks and K_S^0, $\Lambda^0/\bar{\Lambda}^0$
   - Unconstrained vertex fit
   - Mass constrained vertex fit: invariant mass of the di-pion fixed to PDG value of 497.648 MeV and the proton-pion to PDG value 1115.7 MeV
3. Neutral K_S^0, $\Lambda^0/\bar{\Lambda}^0$ track created from the mass-constrained vertex
4. B_d^0, $\Lambda_b^0/\bar{\Lambda}_b{}^0$ reconstruction: three vertex fitting options
   - VKalVrtCascadeFitter: simultaneous fit to two separate vertices, B_d^0 ($\Lambda_b^0/\bar{\Lambda}_b{}^0$) and K_S^0 ($\Lambda^0/\bar{\Lambda}^0$), J/ψ and K_S^0 ($\Lambda^0/\bar{\Lambda}^0$) mass constraints, K_S^0 ($\Lambda^0/\bar{\Lambda}^0$) pointing to the B_d^0 ($\Lambda_b^0/\bar{\Lambda}_b{}^0$) vertex
   - VKalVrtFitter ("Sequential"): neutral K_S^0 ($\Lambda^0/\bar{\Lambda}^0$) trackParticle (from mass constrained V0Hypothesis) plus muon tracks, J/ψ mass constraints
   - CTVMFT ("CDF"): Same as for the VKalVrtCascadeFitter, but, it uses a constant magnetic field and no access to material services
5. Final B_d^0 ($\Lambda_b^0/\bar{\Lambda}_b{}^0$) selection: selection cuts are applied to reduce background

Reconstruction and Selection

Decay Mode	Applied Cuts
Muon selection	STACO muon container is used All Tagged and Combined muons are used Inner detector muon track parameters are used for vertex fitting Muon track must have at least 3 Si hits
Tracks selection	Both tracks have at least one silicon hit Tracks reconstructed using only Transition Radiation Tracker hits are not used Both tracks have $p_T > 100$ MeV
$J/\psi \to \mu\ \mu$	$2.7\ \mathrm{GeV} < M_{\mu\mu} < 3.5\ \mathrm{GeV}$ The vertex fit quality $\chi^2/N_{\mathrm{d.o.f.}} < 200$
$K_S \to \pi^+\ \pi^-$	K_S^0 transverse impact parameter $d_0 < 100$ mm. $440\ \mathrm{MeV} < M_{\pi\pi} < 560\ \mathrm{MeV}$ The invariant mass is reconstructed with an error $\sigma_m < 500$ MeV
$\Lambda^0 \to p^\pm\ \pi^\mp$	$\Lambda^0/\bar{\Lambda}^0$ transverse impact parameter $d_0 < 100$ mm. $1050\ \mathrm{MeV} < M_{p^\pm\pi^\mp} < 1180\ \mathrm{MeV}$ The invariant mass is reconstructed with an error $\sigma_m < 500$ MeV
B_d^0	$5010\ \mathrm{MeV} < M_{B_d^0} < 5605$ MeV Vertex fit $\chi^2/N_{\mathrm{dof}} < 3$ K_S^0, refitted in the B_d^0 fit, must have $p_{\mathrm{T}}^{K_S^0} > 1.5$ GeV Pointing constraint $\cos\theta > 0.999995$
$\Lambda_b^0/\bar{\Lambda}_b^0$	$5320\ \mathrm{MeV} < M_{\Lambda_b^0/\bar{\Lambda}_b^0} < 5920$ MeV Vertex fit $\chi^2/N_{\mathrm{dof}} < 3$ $\Lambda^0/\bar{\Lambda}^0$, refitted in the $\Lambda_b/\bar{\Lambda}_b$ fit, must have $p_{\mathrm{T}}^{\Lambda^0/\bar{\Lambda}^0} > 4$ GeV

K_S^0 and $\Lambda^0/\bar{\Lambda}^0$ Separation

- The transverse momentum p_T of the oppositely charged decay products w.r.t the V^0 is plotted vs the longitudinal momentum asymmetry α

$$\alpha = \frac{q_L^+ - q_L^-}{q_L^+ + q_L^-}$$

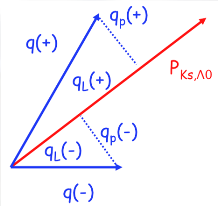

- Hard to distinguish the K_S^0 from the $\Lambda^0/\bar{\Lambda}^0$ in the overlap region $\Rightarrow$ background contribution to the mass distributions

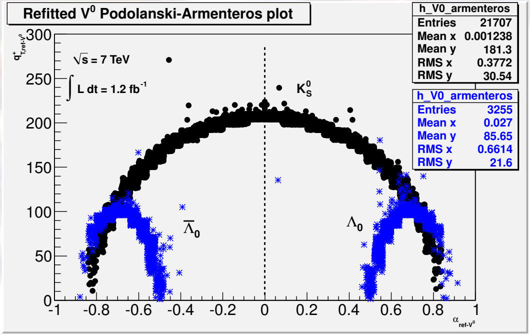

J/ψ, K_S^0 and $\Lambda^0/\bar{\Lambda}^0$ Mass Distributions (MC)

Invariant mass of the mass-unconstrained J/ψ (left), K_S^0 (middle) and $\Lambda^0/\bar{\Lambda}^0$ right

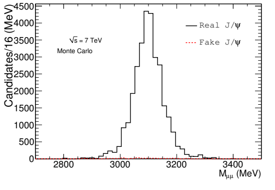

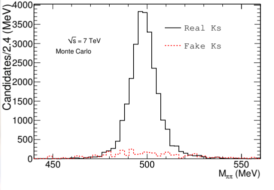

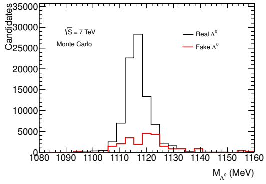

- Only the candidates that passed the final B_d^0, $\Lambda_b/\bar{\Lambda}_b$ selection are shown
- These distributions are affected by B_d^0, $\Lambda_b/\bar{\Lambda}_b$ selection: fake J/ψ, K_S^0 and $\Lambda^0/\bar{\Lambda}^0$ candidates which would otherwise form flat background have a peak-like structure
- In Monte Carlo, most of the selected J/ψ's and large fraction of K_S^0's and $\Lambda^0/\bar{\Lambda}^0$'s are real particles (fraction of fake K_S^0 and $\Lambda^0/\bar{\Lambda}^0$ is $\approx 3\%$)

J/ψ, K_S^0 and $\Lambda^0/\bar{\Lambda}^0$ Mass Distributions (Data)

Invariant mass of the mass-unconstrained J/ψ (left), K_S^0 (middle) and $\Lambda^0/\bar{\Lambda}^0$ right

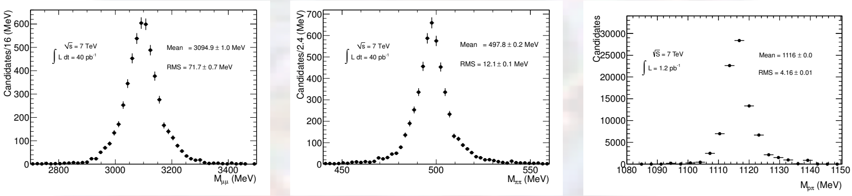

- The mean and RMS of the distributions were calculated
- The mean values agree with the PDG values
- Cut on the invariant mass of J/ψ, K_S^0 and $\Lambda^0/\bar{\Lambda}^0$ does not remove a significant fraction of the signal B_d^0, $\Lambda_b/\bar{\Lambda}_b$ candidates

B_d^0, Λ_b and $\bar{\Lambda}_b$ Invariant Mass Overlap

- The two signal channels have the same decay topology
- Possibility that some of the reconstructed B_d^0 candidates could be misidentified Λ_b or $\bar{\Lambda}_b$ decays
- B_d^0 ($\Lambda_b/\bar{\Lambda}_b$) and K_S^0 ($\Lambda^0/\bar{\Lambda}^0$) invariant masses are calculated assuming $\Lambda_b/\bar{\Lambda}_b$ (B_d^0) and $\Lambda^0/\bar{\Lambda}^0$ (K_S^0) hypotheses
- Misidentified candidates have to be removed from the ML fit.

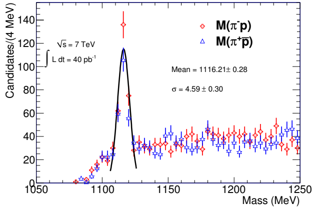

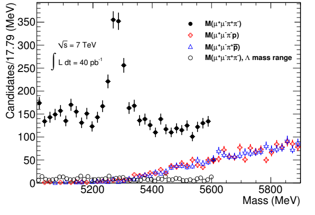

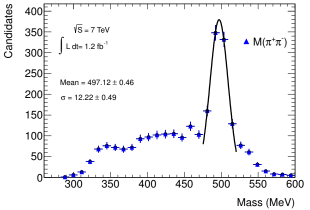

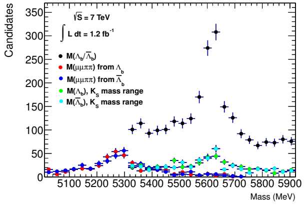

Invariant Mass Fit

- Invariant mass distribution is fitted using extended unbinned maximum likelihood fit to extract the mass and the number of signal/background events
- Likelihood function:

$$\mathcal{L} = \frac{e^{-N_{\rm sig}-N_{\rm bkg}}}{N!} \prod_{i=1}^{N} [N_{\rm sig}\mathcal{M}_{\rm sig}(m_i, \sigma_{m,i}) + N_{\rm bkg}\mathcal{M}_{\rm bkg}(m_i, \sigma_{m,i})] \quad (1)$$

where m_i is the reconstructed mass of the $i^{\rm th}$ candidate, $\sigma_{m,i}$ is its estimated error, $N_{\rm sig}$ and $N_{\rm bkg}$ represent the expected number of signal and background events, and N is the number of reconstructed candidates. $\mathcal{M}_{\rm sig}$ and $\mathcal{M}_{\rm bkg}$ denote probability density functions for the signal and background models

- Signal model: $\mathcal{M}_{\rm sig}(m_i, \sigma_{m,i}) = \frac{1}{\sqrt{2\pi}S_m\sigma_{m,i}} e^{-\frac{(m_i-M)^2}{2S_m^2\sigma_{m,i}^2}}$,

  where M is expected mass and S_m is a scale factor
- Background model:

$$\mathcal{M}_{\rm bkg}(m_i) = \begin{cases} \frac{1}{m_{max} - m_{min}}[1 + b_1(m_i - \frac{m_{max} - m_{min}}{2})] & \text{Linear function} \\ \frac{1}{e^{\frac{(m_i-M)}{\sigma_{m,i}}} + 1} & \text{Bump function} \end{cases} \quad (2)$$

  one free parameter, the slope of the line, b_1
- 5 fitted parameters: M, S_m, N_{sig}, N_{bkg}, and b1

Lifetime Mass Fit

- A simultaneous unbinned maximum likelihood fit to the reconstructed mass and proper decay time is performed

$$\mathcal{L} = \prod_{i=1}^{N} \Big(f_{\rm sig} \mathcal{M}_{\rm sig}(m_i) \tau_{\rm sig}(\tau_i) + (1 - f_{\rm sig}) \mathcal{M}_{\rm bkg}(m_i) \tau_{\rm bkg}(\tau_i) \Big) \quad (3)$$

- The proper decay time PDFs:
  - The signal model is an exponential convoluted with the proper decay time resolution function:

$$\mathcal{T}_{sig}(\tau_i, \sigma_{\tau_i}) = E(\tau^{'}) \otimes R(\tau^{'} - \tau_i, \sigma_{\tau_i}) \times w_{sig}(\sigma_\tau) \quad (4)$$

  - The prompt background: delta function smeared with the resolution function

$$\mathcal{T}_{bkg1}(\tau_i, \sigma_{\tau_i}) = \delta(\tau^{'}) \otimes R(\tau^{'} - \tau_i, \sigma_{\tau_i}) \times w_{bkg}(\sigma_\tau) \quad (5)$$

  - Non-prompt background: sum of two exponential functions convoluted with the resolution function

$$\mathcal{T}_{bkg2}(\tau_i, \sigma_{\tau_i}) = \left[\frac{b}{\tau_{\rm eff1}} exp\left(\frac{-\tau^{'}}{\tau_{\rm eff1}}\right) + \frac{1-b}{\tau_{\rm eff2}} exp\left(\frac{-\tau^{'}}{\tau_{\rm eff2}}\right) \right] \otimes R(\tau^{'} - \tau_i, \sigma_{\tau_i}) \times w_{bkg}(\sigma_\tau) \quad (6)$$

  - background from other sources in data: a symmetric double exponential function and convoluted with the resolution function

$$\mathcal{T}_{\rm bkg3}(\tau_i, \sigma_{\tau_i}) = \frac{1}{2.\tau_{\rm eff3}} exp\left(\frac{-|\tau^{'}|}{\tau_{\rm eff3}}\right) \otimes R(\tau^{'} - \tau_i, \sigma_{\tau_i}) \times w_{bkg}(\sigma_\tau) \quad (7)$$

- Error distributions $w_{sig}(\sigma_\tau)$ and $w_{bkg}(\sigma_\tau)$ are extracted from data

Uncertainty Distribution of the Proper Decay Time

- It is assumed that error distribution $w_{sig}(\sigma_\tau)$ and $w_{bkg}(\sigma_\tau)$ has the same shape for signal and background
- For lifetime error, we do the sideband background subtraction to get signal and background distributions, $w_{sig}(\sigma_\tau)$ and $w_{bkg}(\sigma_\tau)$

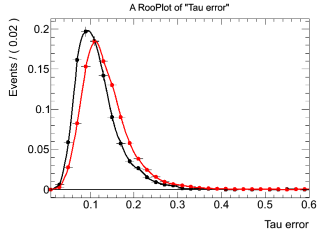

- Events in the sidebands are subtracted from the events in the signal region with weight = $-(1 - f_{sig})N_{sr}/N_{sb}$, where, N_{sr} is the number of events in the signal region, N_{sb} is the number of events in the sidebands, and f_{sig} is the signal fraction in the signal region determined from the mass fit

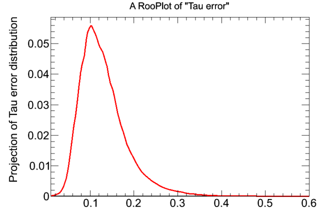

Systematic errors

- Selection Cuts: Cut used in the selection can bias the proper decay time measurements
- Alignment of the Inner Detector: the relative position along the beam line of the Inner Detector modules can give rise of systematics (PV and SV)
- Fitting Models: different models for mass and proper time are tested
- Size of the Mass Range: estimate the effect of any difference due to potential influence of the events at the edge of the mass window
- Choice of Primary Vertex: the method used to select the primary vertex can give systematics errors

Source of systematics	Uncertaintiy on $\tau_{B_d^0}$ (ps)
Selected Cuts	0.010
Alignment of Inner Detector	0.031
Fitting models	-0.017
Size of Mass Range	0.021
Choice of Primary Vertex	–
Total, quadratic sum	0.042